ISBN: 978-3-95450-211-0 doi:10.18429/JACoW-SRF2019-MOP010

AB INITIO CALCULATIONS ON THE GROWTH AND SUPERCONDUCTING PROPERTIES OF NB_3SN*

N. S. Sitaraman†, T. A. Arias, P. D. Cueva, M. M. Kelley, R. D. Porter, Z. Sun,
M. U. Liepe, D. A. Muller, Cornell University Department of Physics, Ithaca, NY14850, USA
J. Carlson, A. R. Pack, M. K. Transtrum,
Brigham Young University Department of Physics, Provo, UT84602, USA

Abstract

In this work, we employ theoretical *ab initio* techniques to solve mysteries and gain new insights in Nb_3Sn SRF physics. We determine the temperature dependence of Nb_3Sn antisite defect formation energies, and discuss the implications of these results for defect segregation. We calculate the phonon spectral function for Nb_3Sn cells with different combinations of antisite defects and use these results to determine T_c as a function of stoichiometry. These results allow for the first-ever determination of T_c in the tin-rich regime, where experimental measurements are unavailable and which is critical to understanding the impact of tin-rich grain boundaries on superconducting cavity performance. Finally, we propose a theory for the growth mechanism of Nb_3Sn growth on a thick oxide, explaining the puzzling disappearing droplet behavior of Sn on Nb oxide and suggesting how in general an oxide layer reacts with Sn to produce a uniform Nb_3Sn layer.

INTRODUCTION

Density Functional Theory (DFT) is a versatile tool that can be used to calculate, without any needed experimental input and to within a few percent accuracy, an incredibly wide of array of fundamental material properties from electronic structure to activation energies to superconducting properties. This makes DFT a very useful complement to experimental research of advanced materials such as those used in SRF cavities. This paper presents pertinent results the on point defects, the growth mechanisms and the superconductivity of Nb_3Sn and the implications of these results to the future of Nb_3Sn SRF cavities [1–4].

CALCULATIONS ON POINT DEFECTS

As part of an in-depth effort to calculate the A15 region of the Nb-Sn phase diagram (which includes Nb_3Sn at 25% Sn), we have gained a rich understanding of the behavior of antisite defects in the material, which are the primary cause of off-stoichiometry. In particular, both kinds of antisite defects dramatically change the Fermi level density of states, which has major implications for their behavior at high temperature during the Nb_3Sn growth process, and at low temperature during cavity operation (discussed in a later section). At the root of this phenomenon is the fact that perfect, stoichiometric Nb_3Sn has a very high Fermi level density of states, a property directly related to its excellent superconducting properties. This means that at high temperatures Nb_3Sn has a very high electronic entropy, and thus very low electronic free energy. Therefore, defects that reduce the Fermi level density of states are significantly less energetically favorable than they would otherwise be.

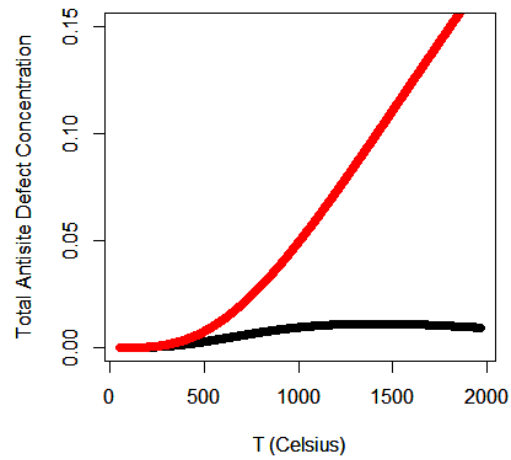

Figure 1: Calculated antisite defect concentrations in 25% Sn Nb_3Sn as a function of temperature, assuming defect formation energies that have been corrected (Black) and have not been corrected (Red) for electronic entropy effects.

In general, electronic entropy increases linearly with temperature, and the corresponding contribution $T \cdot S$ to the free energy increases quadratically with temperature. Because the configurational entropy contribution to the free energy increases only linearly with temperature, the quadratic electronic free energy term dominates at high temperature, preventing defect concentration from growing indefinitely. Using DFT, we calculate antisite defect formation energies at zero temperature, and at the coating temperature of approximately 1200 Celsius. We find that, over this range of temperatures, the free energy for a niobium atom to occupy a tin site increases by 0.24 eV, while the free energy for a tin atom to occupy a niobium site increases by 0.22 eV. Figure 1 shows the impact of these effects on defect concentrations: although zero-temperature defect formation energies would suggest that at the coating temperature nearly 10% of all sites in stoichiometric Nb_3Sn should be occupied by antisite defects, proper accounting of electronic entropy indicates that, actually, only about 1% of all sites are occupied by antisite defects at this temperature.

* This work was supported by the US National Science Foundation under award PHY-1549132, the Center for Bright Beams.
† nss87@cornell.edu

ISBN: 978-3-95450-211-0 doi:10.18429/JACoW-SRF2019-MOP010

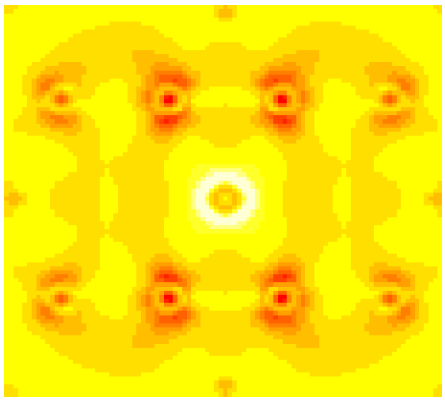

Figure 2: Real-space change in Fermi level density of states due to a niobium-on-tin antisite defect (center). The effect is strongly negative around nearest-neighbor atoms, and still significant for next-nearest-neighbor atoms.

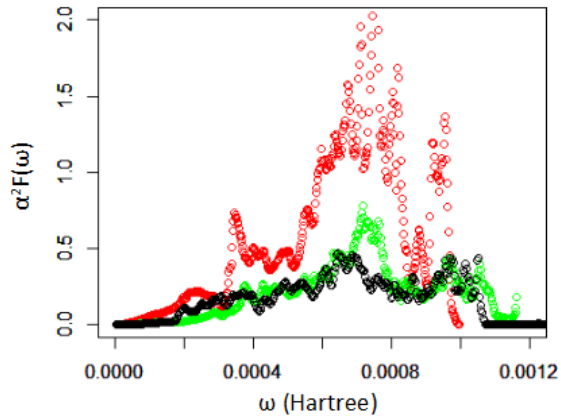

Figure 3: Example Phonon spectral function calculation for stoichiometric (red) tin-poor (green) and tin-rich (black) A15 cells.

The effect of antisite defects on the Fermi level density of states not only determines their equilibrium concentrations, but also determines how they interact with other defects and with each other. In particular, defects that suppress the Fermi level density of states in some volume of radius r (visualized in Fig. 2) can reduce their effect on electronic entropy and lower their free energy by moving within r of other defects or disorder that also reduce the Fermi level density of states. This means that interactions between antisite defects which are strongly repulsive at low temperatures are only mildly repulsive at high temperatures. This effect plays a key role in determining the tin-poor limit of the A15 phase at high temperatures.

Another interesting implication is that antisite defects will tend to be attracted to grain boundaries and dislocations, where Fermi level density of states is lower due to disorder and strain. This is one possible explanation for the observed 3 *nm* sheath of tin-rich stoichiometry observed around grain boundaries in some Nb_3Sn layers [5]. Such Fermi level effects also apply for common impurities such as oxygen, nitrogen, and carbon. Preliminary calculations suggest that these impurities prefer Nb intersitial sites to Nb_3Sn interstitial sites at zero temperature and that this preference gets stronger at high temperature because they tend to suppress the Fermi level density of states in Nb_3Sn. We would therefore expect such impurities to gather near grain boundaries in in Nb_3Sn to the extent that they are present in Nb_3Sn at all.

GRAIN BOUNDARIES AND T_c CALCULATIONS

The most important effect of antisite disorder in Nb_3Sn is to reduce T_c, and thus reduce cavity quality factor and quench field. Measurements have shown that T_c drops from its maximum value of about 18K to 6K at the tin-poor stoichiometry limit of 17-18% Sn [6]. This makes it possible to understand the effect of tin-poor regions on the superconducting properties of the Nb_3Sn layer. Tin-rich stoichiometry has also been observed, but only in nanometer-scale regions around grain boundaries [5]. The properties of tin-rich Nb_3Sn are difficult to measure directly as it only exists in such small regions, but they can be calculated using DFT.

To do this, we calculate electron-phonon scattering amplitudes in A15 cells across the observed stoichiometry range. In order to make these calculations as precise as possible, we employ Wannier function methods to integrate smoothly over all scattering processes in momentum space [7]. These scattering amplitudes are used to calculate the phonon spectral function (Fig. 3), which can be used to estimate T_c using the McMillan formula [8]. We accurately reproduced T_c for bcc niobium as well as the experimentally measured stoichiometry range of the A15 phase, as described in Table 1. For experimentally inaccessible tin-rich stoichiometry, we find that T_c falls to a minimum of about 5K at 31.25% Sn stoichiometry (Fig. 4). This information, taken together with experimental measurements of the stoichiometry profile around grain boundaries from the Seidman group at Northwestern, has enabled simulations of magnetic flux entry at grain boundaries performed by the Transtrum group at Brigham Young (Fig. 5). These simulations show that tin-rich grain boundaries can admit flux vortices even at modest fields, resulting in undesirable Q-slope behavior.

Table 1: Calculated vs. Measured T_c

Composition	Experimental T_c (K)	Calculated T_c (K)
Pure Nb	9.3	10.5
18.75% Sn	6	5.7
20.83% Sn	7.1	5.7
Nb_3Sn	18	17.8

It is important to consider other contributing factors to T_c suppression in grain boundaries, both to accurately predict the overall effect of a tin-rich grain boundary on T_c, and to accurately compare tin-rich grain boundaries to "clean"

ISBN: 978-3-95450-211-0 doi:10.18429/JACoW-SRF2019-MOP010

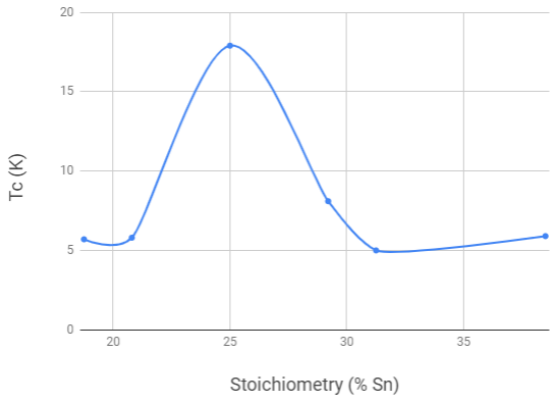

Figure 4: Calculated T_c as a function of stoichiometry, showing a minimum of about 5 Kelvin in the tin-rich regime.

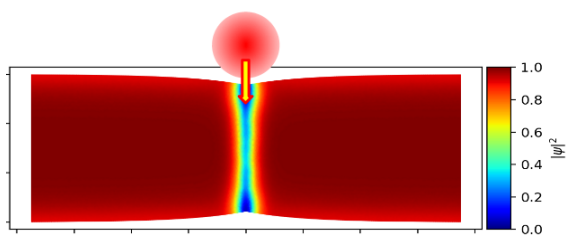

Figure 5: Example simulation of the superconducting order parameter in a tin-rich grain boundary.

25% Sn stoichiometry grain boundaries. While it is difficult to directly calculate T_c for grain boundaries due to their extremely complicated phonon spectra, it is possible to estimate their effect on T_c by calculating their effect on Fermi level density of states (Fig. 6), which we find to be correlated with T_c (Fig. 7). Given this relationship between the Fermi level density of states and T_c, we estimate that a clean grain boundary would suppress T_c by 25% over a core region of 2.2 nm, a mild effect compared to the 70% reduction inflicted by severe off-stoichiometry. We can also estimate the effect of strain on T_c, and we find that it would

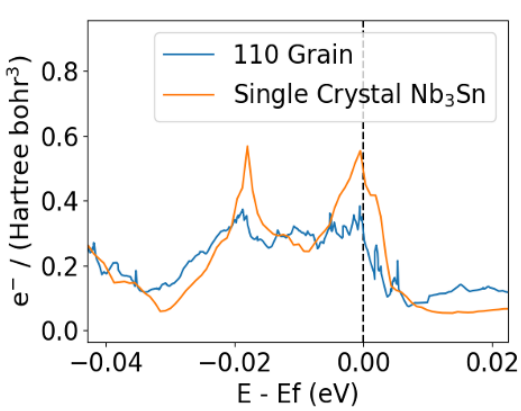

Figure 6: Calculated density of states in bulk Nb_3Sn as contrasted to that in the immediate vicinity of a grain boundary.

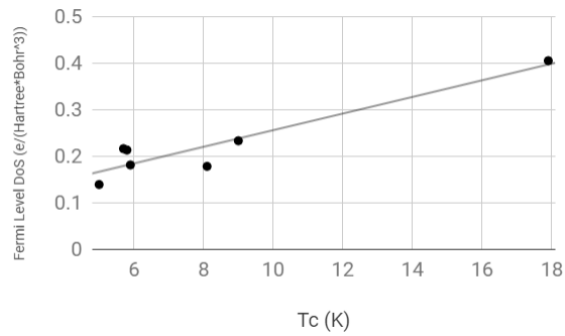

Figure 7: Correlation between T_c and Fermi level density of states in A15 cells of different stoichiometries.

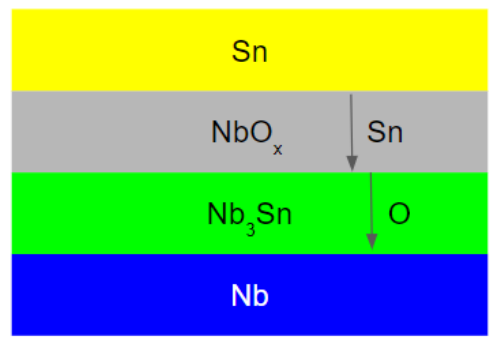

Figure 8: Schematic of the proposed Nb_3Sn growth mechanism, showing the development of a Nb_3Sn layer underneath the oxide along with the relevant diffusion processes.

take a very large 4% strain to reduce T_c by a factor of 2. Given these results, we conclude that clean grain boundaries are likely to result in significantly better cavity performance than dirty grain boundaries. Future experiments and calculations will further elucidate the relationship between grain boundary composition and cavity performance.

NUCLEATION

It has long been known that effective nucleation of Nb_3Sn is an essential step in the growth of a high-quality Nb_3Sn layer. A recent layer growth study by the Liepe group at Cornell showed that some features of finished Nb_3Sn layers, in particular undesirable thin regions, can be traced back to features at the nucleation stage [9, 10]. Specifically, they found that the presence of a thick niobium oxide changed the nucleation process in a beneficial way, leading for more uniform Nb_3Sn. Based on these results, we have developed a new theory for the mechanism of Nb_3Sn growth on an oxidized surface. In this mechanism, illustrated in Fig. 8, tin diffuses through the oxide layer to the bulk niobium interface. There, it interacts with the oxide to produce Nb_3Sn and oxygen intersitials, which diffuse down into the bulk niobium. At the standard nucleation temperature of 500 C, this process is energetically favorable.

In contrast with the growth process of Nb_3Sn on pure Nb, the above process does not involve the diffusion of Sn

ISBN: 978-3-95450-211-0 doi:10.18429/JACoW-SRF2019-MOP010

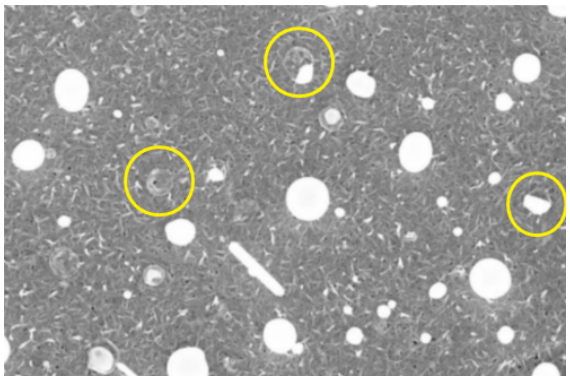

Figure 9: Image of tin droplets on an oxide surface, showing some droplets at various stages of adsorption.

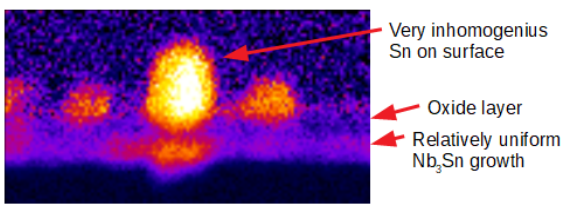

Figure 10: Cross section of nucleated Nb_3Sn layer, showing a relatively uniform layer forming underneath the oxide.

through the growing Nb_3Sn layer. This is important because Sn diffusion through Nb_3Sn is known to be extremely inhomogeneous, occurring almost exclusively along grain boundaries and therefore inevitably leading to inhomogeneities within grains. Depending on the nature of Sn diffusion through niobium oxide and oxygen diffusion through Nb_3Sn, growth on an oxide may in general be more uniform than growth on pure Nb. This appears to be the case for nucleation on niobium oxide. Figure 9 shows that tin droplets on a niobium oxide surface tend to "disappear" from the surface, and Fig. 10 shows that this tin is in fact reacting underneath the oxide. The Liepe group plans to explore the possibility of growing complete Nb_3Sn layers from oxide in the future.

The Liepe group is also exploring the possibility of nucleating Nb_3Sn layers electrochemically [11]. Early results have been promising, showing that under the right conditions of voltage, pH, and surface oxidation, a chemical reaction occurs that strongly binds electroplated tin to the niobium substrate. In theory, it is possible for Sn ions to react with niobium oxide to grow Nb_3Sn from solution, a process that may be sufficiently catalyzed by the solution to grow a substantial Nb_3Sn layer in spite of the low temperature. We have begun calculations using Joint Density Functional Theory to investigate this system in detail (Fig. 11) [12].

CONCLUSIONS

We have demonstrated the fruitful application of DFT to open problems in Nb_3Sn SRF related to point defect behavior, the superconducting properties of grain boundaries, and Nb_3Sn layer nucleation. By improving our understanding

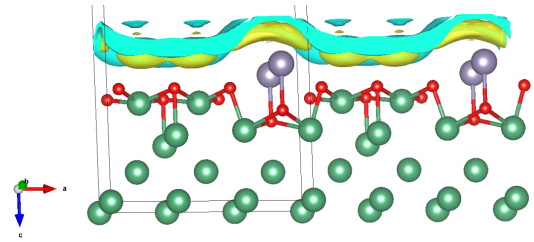

Figure 11: Calculated bound charge density surrounding tin ad-atoms (purple) on a realistic niobium oxide (green and red) surface in aqueous solution.

of the fundamental physics at work, these results will help develop new recipes to maximize cavity Q and quench field.

ACKNOWLEDGMENT

We would like to thank Jae-yel Lee and David Seidman of Northwestern University for sharing their grain boundary segregation measurements with us, and thank Sam Posen of Fermilab for organizing, facilitating, and contributing valuable insights to the many meetings we had with them.

REFERENCES

[1] R. Sundararaman, K. Letchworth-Weaver, K. A. Schwarz, D. Gunceler, Y. Ozhabes and T. A. Arias, "JDFTx: software for joint density-functional theory," SoftwareX 6, 278, 2017

[2] S. Posen, M. Liepe. D. Hall, "Proof-of-principle demonstration of Nb3Sn superconducting RF cavities for high Q0 applications," *Applied Physics Letters*, vol. 106, Issue 8, February 2015. doi:10.1063/1.4913247

[3] R. D. Porter, T. A. Arias, P. D. Cueva, M. Liepe, D. A. Muller, A. R. Pack, N. Sitaraman, M. K. Transtrum, "Field Limitation in Nb3Sn Cavities, 19th International Conference on RF Superconductivity," presented at the SRF'19, Dresden, Germany, Jun.-Jul. 2019, paper THFUA5.

[4] S. Posen and M. Liepe, "Advances in development of Nb3Sn superconducting radio-frequency cavities," *Phys. Rev. ST Accel. Beams*, vol. 15, p. 112001, 2014. doi:10.1103/PhysRevSTAB.17.112001

[5] J. Lee, K. He, Z. Mao, D.N. Seidman, D.L. Hall, M. Liepe, S. Posen, T. Spina, "Performance-Limiting Imperfections in Nb3Sn Coatings for SRF Cavity Applications: Grain Boundary (GB) Segregations," presented at the SRF'19, Dresden, Germany, Jun.-Jul. 2019, paper MOP008.

[6] A Godeke, "A review of the properties of Nb3Sn and their variation with A15 composition, morphology and strain state," *Superconductor Science and Technology*, vol. 19, no. 8, pp. R68–R80, August 2006.

[7] N. Marzari, D. Vanderbilt, "Maximally localized generalized Wannier functions for composite energy bands," *Phys. Rev. B*, vol. 56, p. 12847, November 1997. doi:10.1103/PhysRevB.56.12847

[8] W. L. McMillan, "Transition Temperature of Strong-Coupled Superconductors," *Phys. Rev.*, vol. 167, p. 331, March 1968. doi:10.1103/PhysRev.167.331

ISBN: 978-3-95450-211-0 doi:10.18429/JACoW-SRF2019-MOP010

[9] D. L. Hall, "New Insights into the Limitations on the Efficiency and Achievable Gradients in Nb_3Sn SRF Cavities," Ph.D. Thesis, Physics Department, Cornell Univ., Ithaca, NY, USA, 2017.

[10] R. D. Porter, T. Arias, P. Cueva, D. L. Hall, M. Liepe, J. T. Maniscalco, D. A. Muller, N. Sitaraman, "Next Generation Nb3Sn SRF Cavities for Linear Accelerators", in *Proc. LINAC'18*, Beijing, China, Sep. 2018, pp. 462–465. doi:10.18429/JACoW-LINAC2018-TUPO055

[11] Z. Sun, M. Liepe, R.D. Porter, T. Arias, A.B. Connolly, J.M. Scholtz, N. Sitaraman, M.O. Thompson, X. Deng, K.D. Dobson, "Electroplating of Sn Film on Nb Substrate for Generating Nb-Sn Thin Films and Post Laser Annealing," presented at the SRF'19, Dresden, Germany, Jun.-Jul. 2019, paper MOP014.

[12] R. Sundararaman, K. A. Schwarz, K. Letchworth-Weaver, and T .A. Arias, "Spicing up continuum solvation models with SaLSA: The spherically averaged liquid susceptibility ansatz," *J. Chem. Phys.*, vol. 142, p. 054102, January 2015. doi:10.1063/1.4906828